PRINT ISSN 1119-8362
Electronic ISSN 2659-1502

Full-text Available Online at
https://www.ajol.info/index.php/jasem
http://www.bioline.org.br/ja

J. Appl. Sci. Environ. Manage.
Vol. 26 (9) 1565-1573 September 2022

Analysis of Forest Dynamics using Landscape Metrics and Markov Chain Model in Omo Forest Reserve, Ogun State, Nigeria

MSHELIA, ZH; AIGBOKHAN, OJ; AGBOR, CF

Department of Environmental Modelling and Biometric, Forestry Research Institute of Nigeria, Ibadan, Nigeria.

**Corresponding Author Email: zackmshelia@gmail.com*
Other authors: oseyomon255@gmail.com; Chukwuka_Friday@yahoo.com

ABSTRACT: Forest Canopy density (FCD) is an important index in the assessment and monitoring of forest ecosystems and it is a significant indicator for potential management interventions. The objective of this study was to analyse forest cover and landscape changes with Landsat images of 1990 and 2018 using FCD and Landscape metrics and, Markov Chain and CA-Markov to project the forest cover classes in Omo Forest Reserve. The FCD was obtained from the combination of data from the Advance Vegetation Density index (AVI), Bare soil index (BI), and Forest Shadow Index (FSI). Four categories of change were identified in the reserve, no change, growth, degradation, and deforestation. There was no change in 41798.79ha (44.36%), growth had 22498.11ha (23.87%), degradation with 24916.05ha (26.45%), and deforestation with the least change with 5006.43 (5.32%). Deforestation had the least area coverage with 5006.43 ha. Degradation with a change rate of 0.27 % contributed more in terms of change. There was a slight increase in the values of the three diversity indices (SHDI, SHEI, SIDI) while a high degree of homogeneity is recorded in the no forest class, and the three others classes were fragmented. The 28years projection showed a slight change with no forest area gaining 1.7% while the high forest density losing 2%. Assessment and monitoring of the forest ecosystem will enhance its ecosystem services potential.

DOI: **https://dx.doi.org/10.4314/jasem.v26i9.16**

Cite this paper as: MSHELIA, Z. H; AIGBOKHAN, O. J; AGBOR, C. F. (2022). Analysis of Forest Dynamics using Landscape Metrics and Markov Chain Model in Omo Forest Reserve, Ogun State, Nigeria. *J. Appl. Sci. Environ. Manage.* 26 (9) 1565-1573

Dates: Received: 15 August 2022; Revised: 23 September 2022; Accepted: 26 September 2022

Keywords: Forest Canopy Density; Landscape metrics; Markov chain; Degradation; Fragmentation

The increase pressure on the forests due to significant growth in human disturbance particularly in the tropics has resulted to a consistent degradation of the forest areas (Kiran *et al.*, 2011 and Lewis *et al.*, 2015). It also has an effect on the composition, abundance and natural regeneration of the species (Benitez-Malvido, 1998 and Laurance *et al.*, 2007). Tropical deforestation is considered the major contributor to global environmental change (Blaikie *et al.*, 2015) that poses significant threats to biodiversity, climate and livelihoods (Hartter *et al.*, 2012). Deforestation in Africa's tropics accounted for more than 23% of the global forest loss (Houghton, 2012). Protected areas or forest reserves form the backbone of forest conservation policy in developing countries (Craigie *et al.*, 2010). The forests aid as biodiversity repositories (Li *et al.*, 2009), restrain soil erosion (Nandy *et al.*, 2011), prevent landslides since tree roots bind the soil, regulate air moisture, temperature and mitigate global warming (Cabral *et al.*, 2010) by absorbing 30 percent of CO2 emissions from fossil fuels (Pan *et al.*, 2011). The goods and services provided by forested landscapes are vital for the socio-economic development of human populations (DeFries *et al.*, 2004) and their survival (Ramachandra *et al.*, 2013). On a large scale, more recent changes in land cover are changing the structure of the ecosystem, impacting ecosystem goods and services. This disturbance resulted in forest fragmentation with a mosaic of natural plots surrounded by other land uses (Ramachandra and Kumar 2011). A host of anthropogenic activities, such as tree logging, conversion of forest land to agriculture, intense agricultural practices, forest fire and unplanned infrastructural development have contributed to the disruption of the contiguity of forests in predominantly natural landscapes (Buskirk *et al.*, 2000; Boogaert *et al.*, 2004). A change in forest structure due to forest

**Corresponding Author Email: zackmshelia@gmail.com*

fragmentation has affected its functional capacities, as evidenced by declining water production, carbon sequestration potential and biodiversity. (Diaz *et al.,* 2006; Ramachandra and Kumar 2011). Any landscape is a mosaic of heterogeneous interacting dynamic elements, i.e., the occurrence of natural and anthropogenic processes. A landscape's structure (size, shape and configuration) affects its functional aspects such as biogeochemical cycles and hydrological regimes. Interactions between landscape elements result in a stream of nutrients, minerals and energy that contribute to the functioning of the landscape.

Forest ecosystems constitute a key component of the global carbon cycle that account for over two-thirds of net primary production on land through photosynthesis converting solar energy into biomass (Roy *et al.,* 2001; Ramachandra *et al.,* 2013). Forest ecosystems contain wood and non-timber forest products, such as medicinal resources, firewood and recreational values (Kindstrand *et al.,* 2008). Predicting future spatiotemporal forest scenario of forest degradation and fragmentation is an indispensable need for developing a framework that can help in prioritizing forest conservation aimed at monitoring forest biodiversity loss (Loynl *et al.,*2001), mitigating climate change (Azevedo *et al.,*2014), and gradually improving ecosystem services (Loynl *et al.,*2001). The objective of this study was to analyse forest cover and landscape changes using FCD and Landscape metrics and, Markov Chain and CA-Markov to project the forest cover classes in Omo Forest Reserve.

MATERIALS AND METHODS

Study Area: The Omo Forest Reserve, which derives its name from River Omo that traverses it, is located north of Sunmoge, between latitudes 6º 42' to 7º 05' N and longitude 4º 12' to 4º 35' E (Fig 1) in the Ijebu area of Ogun State in South-western Nigeria. Omo covers about 130,500 hectares, which includes a 460 ha Strict Nature Reserve (Okali and Ola-Adams 1987). The climate is tropical and it is characterized by wet and dry seasons. The temperature ranges between 21 and 34°C while the annual rainfall ranges between 150 and 3000 mm (Larinde *et al.,* 2011; Adedeji *et al.,* 2015). Landsat satellite images of 1990 (Landsat TM) and 2018 (Landsat 8 OLI) with path 190 and row 55, were downloaded from the official website of the United States Geological Survey (USGS). These images provide moderate-scale data of 30m. The satellite images obtained were subjected to basic adjustments or pre-processing. This pre-processing is necessary to adjust the data for use in quantitative analysis (Agbor *et al.,* 2017) and it consists of geometric and radiometric corrections. The images used in this study were first converted to Top of Atmosphere (TOA) radiance using equation 1 (Giannini *et al.,* 2015).

$$L\lambda = \left(\frac{(L_{MAX}\lambda - L_{MIN}\lambda)}{Q_{CAL}\lambda}\right) Q_{CAL} + L_{MIN}\lambda \qquad (1)$$

Where: $L\lambda$ =Spectral radiance at the sensor's aperture [W/(m^2 sr µm)]; Q_{CAL} = Quantized calibrated pixel value [DN]; Q_{CAL}MIN = Minimum quantized calibrated pixel value corresponding to $L_{MIN}\lambda$ [DN]; Q_{CAL}MAX = Maximum quantized calibrated pixel value corresponding to $L_{MAX}\boldsymbol{\lambda}$) [DN]; $L_{MIN}\,\lambda$ = Spectral at-sensor radiance that is scaled to Q_{CAL}MIN [W/(m^2 sr µm)]; LMAX, = Spectral at-sensor radiance that is scaled to Qcalmax [W/ (m 2 sr µm)]

.

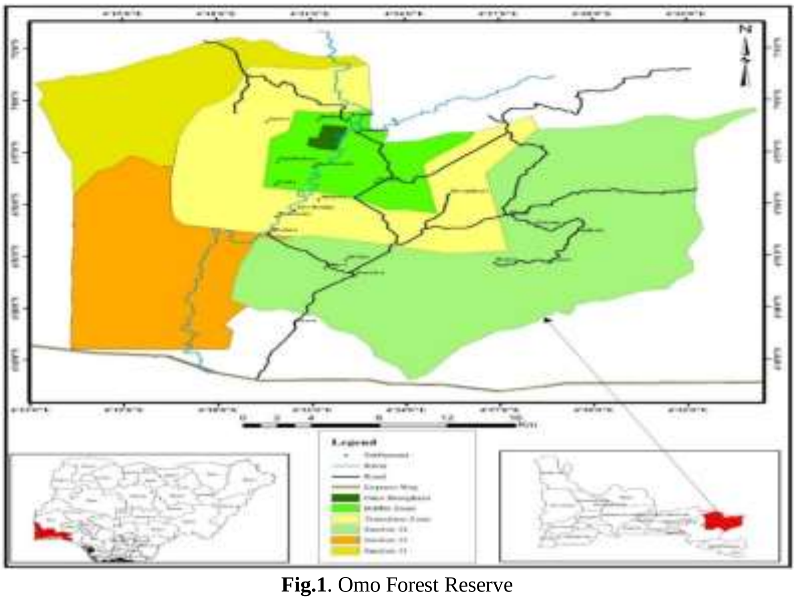

Fig.1. Omo Forest Reserve

The above expression does not consider the atmospheric effects, therefore there is a need to convert images from radiance to reflectance measures, using equation 2 ((Giannini *et al.*, 2015).

$$\rho^{\lambda} = \frac{\pi * TOAr*d^2}{E_{Esun^{\lambda}} * Cos\theta_{sz}} \qquad (2)$$

Where: $\rho\lambda =$ Planetary TOA reflectance (unitless); $\pi=$ mathematical constant approximately equal to 3.14159 (unitless); $L\lambda =$ spectral radiance at the sensors aperture [w/(m^2 sr µm)]; $d^2 =$ the earth-Sun distance (Astronomical unit); $E_{SUN} =$ mean exoatmospheric solar irradiance [w/(m^2 sr µm)]; θ_{SZ}= the solar zenith angle (degree). The cosine of this angle is equal to the sine of the sun elevation $\theta_{SE;}$ That is, $\theta_{SZ} = \cos(90- \theta_{SE})$.

The grid referencing system of individual bands of each of the images used has been transformed to one reference system (WGS1984 UTM Zone 31N). The re-projection is important to make an accurate analysis of the datasets and comparability possible.

Table 1. Landscape metrics used in the study

Metric	Abbreviation	Description
Land Cover	LC	Equals the number of cells for each class based on a classified land cover matrix. The resulting values were multiplied by the cell's value; (ha)
Landscape proportion	LP	Landscape proportion (LP) quantifies proportional abundance of certain class in the total landscape area(0<LP≤100); %
Edge Length	EL	Equals the total length of all patches from a specific class. The resulting values were, of course multiplied with the cell's value; (m).
Edge Density	ED	Edge Density equals the sum of the lengths of all edge segments involving the corresponding patch type, divided by the total landscape area ; (m/ha)
Number of Patches	NP	Express the number of patches identified for each class; (no.).
Patch density	PD	Equals the number of patches of the corresponding patch type divided by total landscape area; (no. /100 ha).
Greatest patch area	GPA	Greatest Patch Area identifies area under single largest patch in a given landscape. It is a measure of dominance i.e. degree of homogeneity
Mean Patch area	MPA	Mean Patch area serves as a fragmentation index. A landscape with smaller mean patch area for the target patch type than another landscape might be considered more fragmented.
Over all Core area	OC	Total core area (ha) or the percentage of the landscape comprised of core area at the class or landscape level. Core area is a compound measure of shape, area and edge depth
Landscape division	LD	Landscape Division is defined as the probability that two randomly chosen places in the landscape to be found in the same patch.
Effective mesh size	m	The probability that two randomly chosen cells are connected (to be included into the same patch); (ha).
Splitting index	S	The number of patches one gets when dividing the total region into parts of equal size in such a way that this new configuration leads to the same degree of landscape division desired; (nr.).
Shannon's Diversity Index	SHDI	Based on information theory; represents the amount of "information" per individual (or patch type, in this case); larger values indicate a greater number of patch types and/or greater evenness among patch types.
Shannon Equitability Index	SHEI	Shannon Equitability (Evenness) Index expresses the dominance of patches within the total area.
Simpson Diversity Index	SIDI	Simpson Diversity Index represents the probability that any two pixels selected at random would be different patch types. The larger the value the greater the likelihood that any 2 randomly drawn cells would be different patch types

Landscape Metrics and Diversity Analysis: Remote Sensing data was primarily utilized to create a necessary database for two time periods, 1990 and 2018. The landscape characterization of the study area will be conducted through a two-stage analysis which will focus on, standardized approach to understand the land cover patterns, and a quantitative approach to describe compositional and spatial aspects of the landscape. In this study, the LecoS plugin in QGIS was used to identify patches by class to calculate landscape metrics. The defined method of landscape ecology indices within landscape structure analysis will be performed for classified classes. Calculated coefficients can be classified according to the type of evaluated characteristic into categories of indices: shape, size, diversity, edges, and proximity (Stejskalova *et al.*, 2012). Statistically, many of the metrics are correlated and can be depicted in concise form according to the structural characteristics (Rajendran *et al.*, 2015). Table 1 shows the indices, acronyms used, and a short description of each indicator.

The CA-Markov Chain Model (CA-MCM): The integration of the CA-Markov model is considered to be valuable for modeling land use changes and able to simulate and predict changes (Singh *et al.*, 2015, Parsa *et al.*, 2016). The CA-Markov model is the combination of Cellular Automata and transition probability matrix generated by the crosstabulation of two different images (Singh *et al.*, 2015). This combination of the CA-Markov model provides a robust approach in Spatio-temporal dynamic modeling (Hamad *et al.*, 2018, Wang *et al.*, 2001). Furthermore, CA uses Markov to add spatial character to the model. In other words, the CA-Markov chain can simulate two-way transitions among any number of categories and can predict any transition among any number of categories (Pontius *et al.*, 2005, Ye *et al.*, 2008).

RESULTS AND DISCUSSION

Forest Canopy Density of Omo Forest Reserve: The AVI and BSI both had a negative relationship with each other, a high AVI value shows high vegetation vigour, and similarly, high BSI shows soil exposure.

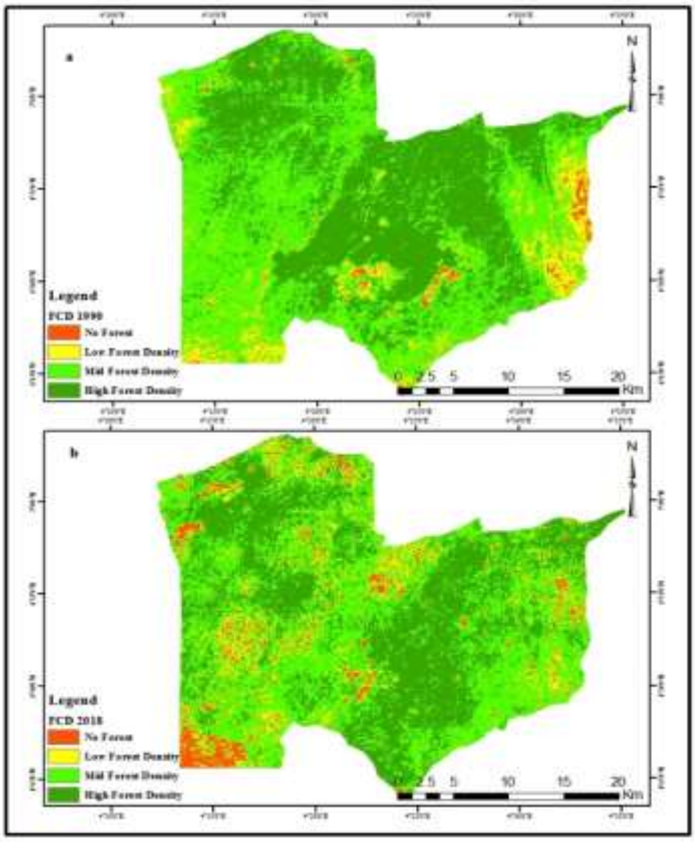

Fig 2. Forest Canopy Density of Omo Forest Reserve 1990 and 2018

Utilising the various spectral indices, vegetation density, and scale shadow index, the forest canopy density map was produced for the years 1990 and 2018. It was thereafter utilised for the classification of the forest cover and its change detection. Based on the percentage, each pixel was classified into four classes of forest canopy density: high forest density, mid forest density, low forest density, and no forest. High forest density is areas having a value from 71 to 100%. In the same manner, 41 – 70%, 5 – 40%, and below 5% were areas with mid forest density, low forest density, and no forest respectively (Figure 2). The maps described the distribution of forest resources in Omo Biosphere through the FCD model. The statistics in Table 2 showed that from 1990 to 2018, the no forest area increased by 3747.42 ha at the rate of 0.14 %. This increase was significant compared to the biosphere that was highly restricted. The changes in low forest area were insignificant as the difference between 1990 and 2018 was 423.99 ha compared to the total land area (94219.38 ha). The mid forest density like the low forest density had an insignificant increase as it was 44.5 % in 1990 and 44.85 % in 2018. The high forest density decreases by 4502.61 ha from 43.78 % in 1990 to 39 % in 2018. The result showed that the rate of forest degradation is more than deforestation in Omo forest reserve. This is a result of logging and farming that takes place in the forest reserve. Even though, the entire Omo forest reserve was accessible except the biosphere it still has great capacity to sink carbon to mitigate the impact of climate change. Krug, (2019) observed that forest management increase biomass accumulation and CO_2 sequestration. Forest management in the observed beech-dominated forest stands leads to a 15.6% higher cumulative biomass growth compared to stands where management was discontinued and when harvested biomass is considered. The cumulative biomass growth of beech alone is noted as about 19.1% higher in management areas than in adjacent forest reserves. The comparison of the selected forest reserves and adjacent management areas to a larger extent (about 450 ha beech-dominated forests) allows this conclusion for the observed stand age classes (Krug, 2019). There is a need to properly manage the existing reserves and create new ones to effectively achieve the benefits of the conversed forest in South Western Nigeria.

Landscape Metrics and Diversity Analysis: Tables 5 showed the values resulting from the calculation of global indices performed for the two periods. In terms of diversity, there was a slight increase of the values of the three indices (SHDI, SHEI, and SIDI) in the reserve

(Table 5), as a result of the increase of some classes area reported to the general distribution of the landscape. The slight increase of the diversity values can be explained by an increase in the No Forest class from 2.13% to 6.11% and a decrease of the High Forest Density class from 43.78% to 38.99% (Table 2).

Table 2. Area of Forest Density Classes of Omo Forest Reserve

Class	1990 Area (ha)	%	2018 Area (ha)	%	Area Diff. (ha)	Change Rate (%)
No Forest	2009.7	2.133	5757.12	6.1103	3747.42	0.142
Low Forest Density	9036.54	9.591	9460.53	10.041	423.99	0.0161
Mid Forest Density	41926.23	44.499	42257.43	44.85	331.2	0.0126
High Forest Density	41246.91	43.778	36744.3	38.999	-4502.61	0.1707
Total	94219.38	100	94219.38	100		

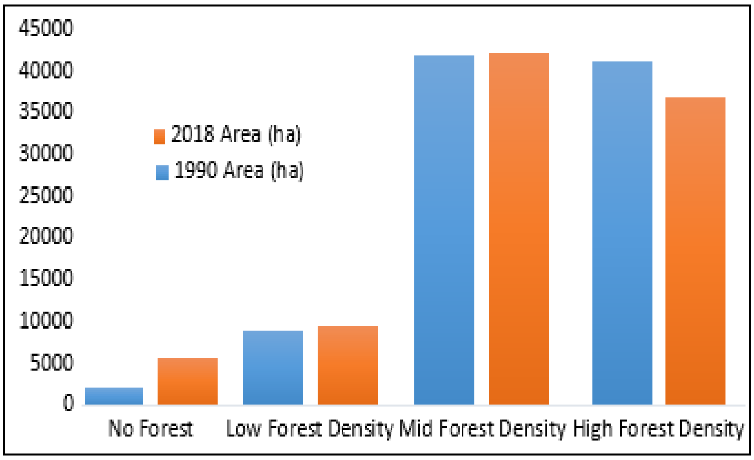

Fig 3. Area of Forest Density Classes of Omo Forest Reserve

However, the values of diversity and evenness remain relatively high, suggesting that the study area, which has favourable physical and geographical conditions, has a complex landscape with certain dominant species. In terms of landscape configuration, features, and functionality, some other landscape indices were calculated (Tables 6). Unlike diversity indices, these were applied particularly to each class. Table 1 presents the indicators, the abbreviation used, and a short description for each type. Land Cover (LC) and Landscape Proportion (LP) - Significant changes were observed in the four classes both in the high forest density classes. The *edge length (EL)* and *edge density (ED)* - The result showed an increase of the two indices values for most classes tending towards heterogeneity.

Number of Patches (NP) and *Patch Density (PD)* - A significant decrease was observed in mid forest density (MFD) of the biosphere from 120 to 47. This explained why MFD occupied 49% of the biosphere. All the classes in Omo Forest Reserve had a decrease in PD except the no forest. Patch Density reflects the extent of landscape fragmentation and is therefore crucial for landscape structure assessment. Comparison of classes with varying sizes showed decreasing PD in most of the classes in the reserve. However, the rate of the decrease is moderate, thereby making the level of fragmentation insignificant for now. It was further explained following also the values of edge density. *Edge density*, with *patch number* and *patch density*, are representative for establishing the *fragmentation degree* of the landscape. The values obtained for the fragmentation (NP and, consequently, PD and ED) reveal a decrease in the study area's fragmentation degree, inducing a clustering tendency.

Greatest patch area (GPA) is related to the *degree of homogeneity or dominance* of the landscape. Omo forest reserve had the highest GPA in MFD with 346554000 m in 1990 and 235075500 m in 2018. *The mean patch area* is also higher for the categories mentioned above.
Landscape division, Effective mesh size, and Splitting index (LD, m, and s) are interconnected and measure the fragmentation degree of the landscape. They have the advantage, unlike other conventional indicators, that any omissions or additions of other small-sized patches do not influence the final result.

In this study, values of LD for all classes are high (above 0.9), reflecting a high degree of fragmentation of class types. Although landscape division and Mesh are perfectly correlated, but inversely, both metrics are included because of the differences in units and interpretation. Split (s) is based on the cumulative patch area distribution, and is interpreted as the effective mesh number, or some patches with a constant patch size when the corresponding patch type is subdivided into S patches, where S is the value of the splitting index (McGarigal *et al.*,2002).

Jaeger 2000, defines the splitting index as the number of patches that resulted after dividing the total area into equal size parts so that this new configuration leads to the same degree of landscape division (LD).

Table 6. Landscape Metrics Computed for Class Types for 1990 and 2018 in Omo Forest Reserve

Class	LC (m)	LP (%)	EL (m)	ED	NP	PD	GPA (m)	MPA (m)	LD	m (m)	S
NF 1990	20097000	0.013	1089060	0.0007	2632	1.68E-06	1948500	7636	1	4476.211	349995.2
NF 2018	57571200	0.037	2185920	0.0014	4670	2.98E-06	11492100	12328	1	91449.85	17131.27
LFD 1990	90365400	0.058	5694720	0.0036	12052	7.69E-06	23572800	7498	1	392418.4	3992.30
LFD 2018	94605300	0.06	6372720	0.0041	11954	7.63E-06	3006000	7914	1	14244.94	109979.55
MFD 1990	419262300	0.268	16507800	0.0105	13186	8.42E-06	346554000	31796	0.95	76674563	20.432
MFD 2018	422574300	0.27	13663860	0.0087	7145	4.56E-06	235075500	59143	0.97	43089790.89	36.36
HFD 1990	412469100	0.263	11849580	0.0076	13972	8.92E-06	233640000	29521	0.97	41169625	38.054
HFD 2018	367443000	0.235	8817180	0.0056	8547	5.46E-06	167281200	42991	0.99	23271972.59	67.32

When its value is 1, the landscape is represented by a single patch, the value increasing as the landscape is divided into several patches. Considering these aspects, the interpretation of the results must take into account the correlation of these three complementary indicators.

Table 5. Landscape Diversity Indices between 1990 and 2018 of Omo Forest Reserve

Metric	1990	2018
Shannon's Diversity Index	1.292	1.352
Shannon Equitability Index	0.803	0.839
Simpson Diversity Index	0.697	0.708

The resulting values of the three indicators suggest different degrees of fragmentation for each class. Thus, the areas with a high degree of homogeneity are represented was recorded in the no forest class, and the three others classes were fragmented. The degree of landscape fragmentation is an important environmental indicator in the fields of biodiversity and sustainable development. In addition, information on the degree of landscape fragmentation is relevant in regional planning and for decisions about infrastructure placement or removal. Its analysis of different time series shows how strong the current trends are and what their direction is (Jaeger *et al.*, 2006).

Transition probability matrix: Tables 7 showed the transition probability matrix computed using the forest cover classes in Omo Biosphere and Omo Forest Reserve of the periods of 1990-2018 to show the projection of each forest cover class category. This procedure contains two significant matrices of probabilities, which are the transition probability matrix and the conditional probability images. The probability maps generated by the Markov model convey initial information on the likelihood of forest cover change occurrence before the final CA–Markov model (Figure 5). The probability matrix for forest cover conversions for all classes in Omo Forest Reserve is shown in Table 7. The probability of change for no forest class to no forest is 31.75%, no forest to low forest density is 19.36%, no forest to mid forest density is 31.73% and no forest to high forest density is 17.16%. The probability of change for high forest density to no forest is 3.29%, high forest density to low forest density is 8.88%, high forest density to mid forest density is 47.4% and high forest density to high forest density is 40.43%. The result of the transition probability matrix showed that transition from no forest to low forest, mid forest, and high forest densities are faster if the current trend of change continues as compared to the forest degrading from high and mid forest densities to low forest density and no forest class in 2046. This showed that the forest reserve can regenerate despite the level of degradation if properly managed. The result of the 28years projection in Omo Forest Reserve (Table 8) showed a slight change with no forest area gaining 1550.7 ha from 6.1% to 7.8% while the high forest density degraded from 39% in 2018 to 37% in 2046, which is 1760.4 ha. It is important to know, that forests with a good management system will serve as a carbon sink for climate change mitigation. Hence, there is a need for yearly monitoring of the reserve to fulfill it role of sinking carbon and providing ecosystem services. Projecting Omo Forest Reserve showed the potential of the reserve to maintain biodiversity and to sink carbon. Projection can also show the state of forest degradation. Therefore, projection is very important for decision-making to achieve sustainable forest management.

Table 7. Transition Probability Matrix of Omo Forest Reserve for 28 years

Class	No Forest	Low Forest Density	Mid Forest Density	High Forest Density
No Forest	0.3175	0.1936	0.3173	0.1716
Low Forest Density	0.1586	0.1314	0.5036	0.2063
Mid Forest Density	0.0656	0.1216	0.4061	0.4067
High Forest Density	0.0329	0.0888	0.474	0.4043

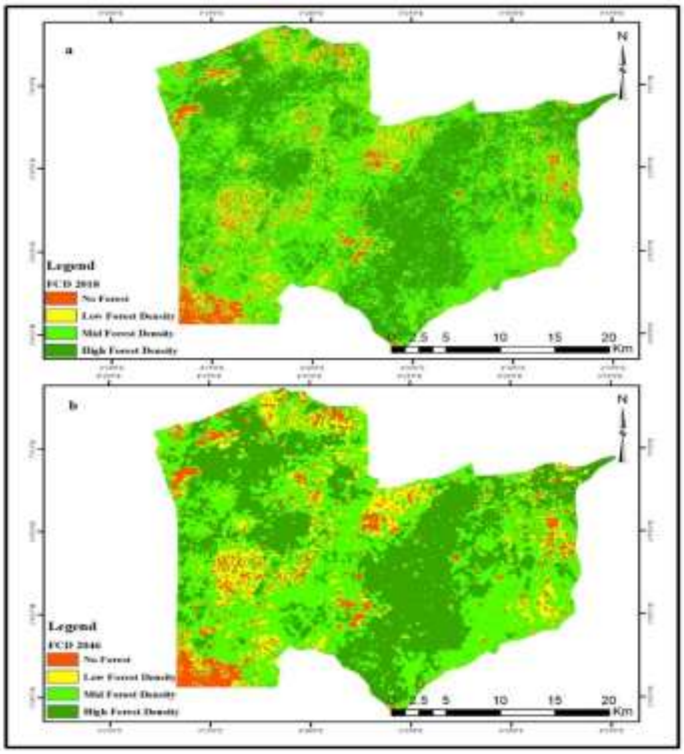

Fig 4: Forest Cover of Omo Forest Reserve 2018 (a) and 2046 (b)

Table 8. Area of Forest Cover of Omo Forest Reserve for 2018 and 2046

Class	2018 Area (ha)	%	2046 Area (ha)	%
No Forest	5757.12	6.1	7307.82	7.8
Low Forest Density	9460.53	10	10756.53	11
Mid Forest Density	42257.43	45	41171.13	44
High Forest Density	36744.3	39	34983.9	37
Total	94219.38	100	94219.38	100

Conclusion: The study area, which has favourable physical and geographical conditions, has a complex landscape with certain dominant types. The study determined that the diversity and fragmentation model are important for analysing the Spatio-temporal condition of the forest which will help forest managers in decision making, monitoring biodiversity, and conversation planning for sustainable forest management.

REFERENCES

Adedeji, OH; Tope-Ajayi, O.O., & Abegunde, O.L. (2015). 'Assessing and Predicting Changes in the Status of Gambari Forest Reserve, Nigeria Using Remote Sensing and GIS Techniques. *J. Geographic Information System*, 7, 301-318.

Agbor, C. F., Pelemo O. J., Aigbokhan, O. J., Osudiala, C. S. and Alagbe, J. (2017). Forest Loss Assessment in South-West Nigeria Using Geospatial Technologies. *Inter. J. Appl. Res. Technol. 6(3*): 45 – 52.

Akike, S. and Samanta, S. (2016) Land Use/Land Cover and Forest Canopy Density Monitoring of Wafi-Golpu Project Area, Papua New Guinea. *J. Geosci. Environ. Protect.* **4**, 1-14.

Andre B.L., Miller, J., Ahern, J., McGarigal, K., (2012) Measuring Landscapes: A Planner's Handbook, Island Press.

Azevedo, J.; Perera, A.H.; Pinto, M.A. (2014) *Forest Landscapes and Global Change: Challenges for Research and Management*; Springer: Berlin, Germany.

Azizia, Z., Najafi, A. and Sohrabia, H. (2008) Forest Canopy Density Estimating, Using Satellite Images. 21st International Society for Photogrammetry and Remote Sensing (ISPRS), Congress, Beijing, Vol. 37, Part B8, 1127-1130.

Banerjee, K., Panda, S., Bandyopadhyay, J. and Jain, M.K. (2014) Forest Canopy Density Mapping Using Advance Geospatial Technique. *Inter. J. Innov. Sci. Engineer Technol.* 1: 358-363.

Benitez-Malvido, J. (1998) Impact of forest fragmentation on seedling abundance in a tropical rain forest. *Conserv. Biol.*, *12*, 380–389.

Biradar, C.M., Saran, S., Raju, P.L.N. and Royb, P.S. (2005) Forest Canopy Density Stratification: How Relevant Is Biophysical Spectral Response Modelling Approach? *Geocarto International*, 20, 1-7.

Blaikie, P. and Brookfield, H. (2015) Land Degradation and Society. Routledge.

Bonino, E.E. (2006): Changes in carbon pools associated with land-use gradient in the dry Chaco, Argentina. *Forest Ecology and Manage.* 223: 183-189.

Boogaert J, Ceulemans R, Salvador-van ED (2004) Decision tree algorithm for detection of spatial processes in landscape transformation. *Environ Manage.* 33:62–73

Burnham, B.O. (1973) Markov intertemporal land use simulation model. *J. Agric. Appl. Econ.* 5, 253–258.

Buskirk S, William H, Federick R, Smith W, Richard Knight L (2000) An Overview of Forest Fragmentation in the Southern Rocky Mountains 3-14. In: Richard LK, Frederick SW, Steven BW, William RH, William BBL(ed) Forest Fragmentation in the Southern Rocky Mountains, University Press of Colorado, Colorado

Camara, M.; Jamil, N.R.B.; Abdullah, A.F.B.; Hashim, R.B., (2020). Integrating cellular automata Markov model to simulate future land use change of a tropical basin. *Global .J. Environ. Sci. Manage.* 6(3): 403-414.

Chelaru D.A., Oiste A.M., Mihai, F.C., (2014) *Quantifying the changes in landscape configuration using open source GIS. Case study: Bistrita subcarpathian valley, Romania*, 14th International Multidisciplinary Scientific GeoConference on ecology, economics, education and legislation SGEM 2014, Conference Proceedings. 1: 557 – 565.

Craigie, I.D., Baillie, J.E., Balmford, A., Carbone, C., Collen, B., Green, R.E. and Hutton, J.M. (2010) Large Mammal Population Declines in Africa’s Protected Areas. *Biological Conservation.* 143, 2221-2228.

D Behera, M.; Borate, S.N.; Panda, S.N.; Behera, P.R.; Roy, P.S. (2012) Modelling and analyzing the watershed dynamics using Cellular Automata (CA)-Markov model—A geo-information based approach. *J. Earth Syst. Sci*. 121, 1011–1024.

De Groot, R.S.; Wilson, M.A. and Boumans, R.M. (2002): A typology for the classification, description and valuation of ecosystem functions, goods and services. Special Issue: The dynamics and value of ecosystem services: integrating economic and ecological perspectives. *Ecol. Econ.* 41: 393–408.

DeFries R, Foley J, Asner G (2004) Land-use choices: balancing human needs and ecosystem function. *Front Ecol. Environ* 2(5):249–257

Diaz S, Fargione J, Chapin F, Tilman D (2006) Biodiversity loss threatens human well-being. PLoS Biol 4(8):277, 1300-1306

Hamad, R., Balzter, H. and Kolo, K. (2018) Predicting Land Use/Land Cover Changes Using a CA-Markov Model under Two Different Scenarios. Sustainability 10, 3421;

Hartter, J., Ryan, S.J., Diem, J., Palace, M. and Chapman, C.A. (2012) Population, Environment, and Climate in the Albertine Rift: Understanding Local Impacts of Regional Change. AGU Fall Meeting Abstracts, p 0737.

Haygarth, P.M. and Ritz, K. (2009): “The future of soils and land use in the UK: Soil systems for the provision of land-based ecosystem services”. *Land Use Policy*, 26, pp. 187–197.

Houghton, R. (2012) Carbon Emissions and the Drivers of Deforestation and Forest Degradation in the Tropics. *Curr. Opinion in Environ. Sustain.* 4, 597-603.

Jaeger J.A.G. (2000) Landscape division, splitting index, and effective mesh size: new measures of landscape fragmentation. *Landscape Ecol.* 15 (2). 115-130.

Jaeger J.A.G., Esswein H., Schwarz-Von Raumer H.G. (2006) Measuring Landscape Fragmentation with the Effective Mesh Size meff, Zurich.

Kindstrand C, Norman J, Boman M, Mattsson L (2008) Attitude towards various forest functions: a comparison between private forest owners and forest officers. *Scand. J. Forest. Res*. 23:133–136

Kiran, G.S.; Malhi, R.K.M. Economic valuation of forest soils. Curr. Sci. 2011, 100, 396–399.

Kirschbaum, M.U. (2003): “To sink or burn? A discussion of the potential contributions of forests to greenhouse gas balances through storing carbon or providing biofuels”. Biomass and Bioenergy, 24, pp. 297–310.

Kumar, M.; Kumar, P. (2008): “Valuation of the ecosystem services: A psycho-cultural perspective”. Ecological Economics, 64, pp. 808–819.

Kumar, S.; Radhakrishnan, N.; Mathew, S. (2014) Land use change modelling using a Markov model and remote sensing. Geomat. Nat. Hazards Risk 5, 145–156.

Laurance, W.F.; Nascimento, H.E.; Laurance, S.G.; Andrade, A.; Ewers, R.M.; Harms, K.E.; Luizao, R.C.; Ribeiro, J.E. (2007) Habitat fragmentation, variable edge effects, and the landscape-divergence hypothesis. *PLoS ONE 2*, e1017.

Lewis, S.L.; Edwards, D.P.; Galbraith, D. (2015) Increasing human dominance of tropical forests. *Sci.* 349, 827–832.

Li M, Huang C, Zhu Z, Wen W, Xu D, Liu A (2009) Use of remote sensing coupled with a vegetation change tracker model to assess rates of forest change and fragmentation in Missipi, USA. *Int J Remote Sens* 30:6559–6574

Liping, C.; Yujun, S.; Saeed, S., (2018). Monitoring and predicting land use and land cover changes using remote sensing and GIS techniques—A case study of a hilly area, Jiangle, China. PLoS One, 13: e0200493.

Loynl, R.H.; McAlpine, C. Spatial Patterns and Fragmentation: Indicators for Conserving Biodiversity in Forest. *Criteria Indic. Sustain. Manage. 7*, 391.

Manrique, S. M., Núñez, V. Franco, J. (2012): Estimating aboveground biomass in native forest using remote sensing data combined with spectral radiometry. *GeoFocus (Artículos)* 12: 349-373.

McGarigal, K., SA Cushman, Mc Neel, & E Ene (2002). -FRAGSTATS v3: Spatial Pattern Analysis Program for Categorical Maps. Computer software program produced by the authors at the University of Massachusetts, Amherst.

Mishra, V.N.; Rai, P.K.; Mohan, K. (2014) Prediction of land use changes based on land change modeler (LCM) using remote sensing: A case study of Muzaffarpur (Bihar), India. J. Geogr. Inst. Jovan Cvijic SASA 64, 111–127

Nandy S, Kushwaha SPS, Dadhwal VK (2011) Forest degradation assessment in the upper catchment of the river Tons using remote sensing and GIS. *Ecol. Ind.* 11:509–513

Okali, D.U.U. and Ola-Adams, B.A. 1987. Tree population changes in treated rain forest at Omo Forest Reserve, Nigeria. *J. Tropical Ecol.* 3:291-313.

Pan Y, Birdsey RA, Fang J, Houghton R, Kauppi PE, Kurz WA, Phillips OL, Shvidenko A, Lewis SL (2011). A large and persistent carbon sink in the world's forests. *Sci.* 333(6045):988–993

Parsa, V.A.; Yavari, A.; Nejadi, A. (2016) Spatio-temporal analysis of land use/land cover pattern changes in Arasbaran Biosphere Reserve: Iran. Model. *Earth Syst. Environ.* 2, 1–13.

Pătru-Stupariu, I., Stupariu, M. S., Cuculici R. & Huzui, A. (2011) Application of theglobal indicators to landscape change modeling on Prahova Valley (Romanian Carpathians and Subcarpathians), International Journal of the Physical Sciences, vol.6(3), pp. 534-539.

Pontius, G.R.; Malanson, J. (2005) Comparison of the structure and accuracy of two land change models. *Int. J. Geogr. Inf. Sci.* 19, 243–265.

Rajendran, P. and Mani, K. (2015) Quantifying the Dynamics Of Landscape Patterns n Thiruvananthapuram Corporation Using Open Source GIS Tools. International Journal of Research in Engineering and Applied Sciences

Ramachandra TV, Kumar U (2011) Characterisation of landscape with forest fragmentation dynamics. *J. Geogr Inf Syst* 3(03):242

Ramachandra TV, Subash Chandran MD, Bhat SP, Aithal BH, Rao GR, Vishnu M (2013) Status of forest in Shimoga district, Karnataka, Sahyadri conservation series 23, ENVIS Technical Report: 53. ENVIS- Environmental Information System, Centre for Ecological Sciences, Indian Institute of Science, Bangalore

Rikimarku, A., Roy, P. and Miyatake, S. (2002) Tropical forest cover density mapping. *Trop. Ecol.* 43(1): 39-47, 2002.

Rikimaru, A. (1996). LANDSAT TM Data Processing Guide for forest Canopy Density Mapping and Monitoring Model. ITTO workshop on utilization of remote sensing in site assessment and planning for rehabilitation of logged-over forest. Bangkok, Thailand, pp.1-8, July 30-August 1996.

Roy J, Saugier B, Mooney HA (2001) Terrestrial global productivity. Academic, London

Saei jamalabad, M., Abkar, A.A., (2000) Vegetation Coverage Canopy Density Monitering, Using Satellite Images. *ISPRS Commission VII, 17, Amsterdam, Holland*

Singh, S.K.; Mustak, S.; Srivastava, P.K.; Szabó, S.; Islam, T. (2015) Predicting spatial and decadal LULC changes through cellular automata Markov chain models using earth observation datasets and geo-information. *Environ. Process*. 2, 61–78.

Subedi, P.; Subedi, K.; Thapa, B. (2013) Application of a hybrid cellular automaton-Markov (CA-Markov) Model in land-use change prediction: A case study of saddle creek drainage Basin, Florida. *Appl. Ecol. Environ. Sci.* 1: 126–132.

Subedi, P.; Subedi, K.; Thapa, B. Application of a hybrid cellular automaton-Markov (CA-Markov) Model in Thornley, J.H. and Cannell, M.G. (2000): "Managing forests for wood yield and carbon storage: a theoretical study". *Tree Physiology*. 20: 477–484.

Wang, Y.; Zhang, X. (2001) A dynamic modeling approach to simulating socioeconomic effects on landscape changes. *Ecol. Model.* 140, 141–162.

Wang, Z. and Brenner, A. (2009). An Integrated Method for Forest Canopy Cover Mapping Using LANDSAT ETM+ Imagery. *ASPERS/MAPRS* 2009 *Fall Conference*, San Antonio, 16-19 November 2009, 1-8.

Weng, Q. (2002) Land use change analysis in the Zhujiang Delta of China using satellite remote sensing, GIS and stochastic modelling. *J. Environ. Manage*. 64, 273–284.

Ye, B.; Bai, Z. (2008) Simulating land use/cover changes of Nenjiang County based on CA-Markov model. *Comput. Comput. Technol. Agric*. 1, 321–329.